

Supporting Information

Development of a human vasopressin V_{1a}-receptor antagonist from an evolutionary-related insect neuropeptide

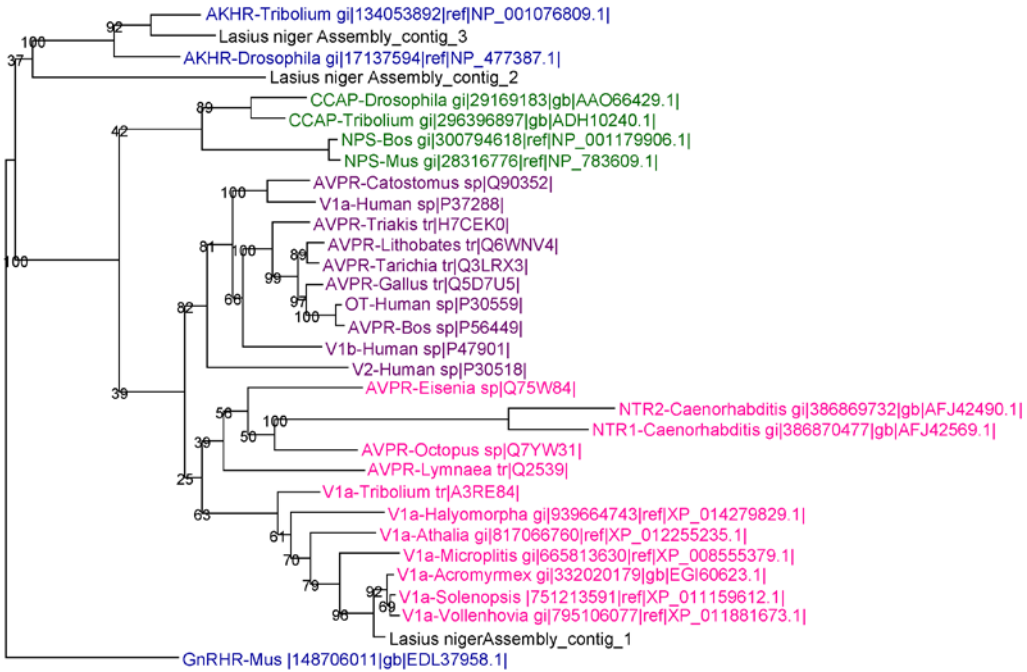
Deleted: From ants to man:

Deleted: Engineering a human vasopressin V_{1a}R-antagonist via an evolutionary strategy

Maria Giulia Di Giglio, Markus Muttenthaler, Kasper Harpsøe, Zita Liutkeviciute, Peter Keov, Thomas Eder, Thomas Rattei, Sarah Arrowsmith, Susan Wray, Ales Marek, Tomas Elbert, Paul F. Alewood, David E. Gloriam and Christian W. Gruber

15 **Supplementary Figures**

16
17



18
19

20 **Supplementary Fig. 1. Phylogenetic tree of oxytocin/vasopressin (OT/AVP) receptors.**
 21 Published invertebrate and vertebrate receptors were used together with the top three blast hits from
 22 the *L. niger* transcriptome (*Lasius niger* Assembly contigs_1-3, shown in black) to reconstruct the
 23 phylogenetic relationship. Only the best blast hit of *L. niger* (*Lasius niger* Assembly contig_1)
 24 clusters together with OT/AVP receptors in the same branch, while the other two hits cluster with
 25 invertebrate adipokinetic hormone receptors (AKHR). Vertebrate OT/AVP receptors are shown in
 26 violet and invertebrate OT/AVPR receptors are shown in pink. Putative OT/AVP-like ant receptors
 27 are shown in pink. Vertebrate neuropeptide S receptors (NPSR)/invertebrate crustacean
 28 cardioactive peptide receptors (CCAPR) are shown in green and vertebrate gonadotropin-releasing
 29 hormone receptors (GnRHR)/invertebrate AKHR are shown in blue. According to the study of Pitti
 30 and Manoj¹ the mouse gonadotropin-releasing hormone receptor (GnRHR) was used as outgroup.
 31 Numbers at nodes indicate confidence values and ExpASY/Genbank entry IDs of sequences are
 32 listed next to the receptor names.

33

```

Lasius INTR      1  -----MSYDSNTSL-----SPSSLSSSMETFDLIRDFNLARVEIAVITL
Tribolium INTR  1  -----MD-----ISEN-----STYLFDKHEDRNNTDRDENLARVEIATLAI
Human V2R       1  MLMAST-----TSAVPGHPSLPSLPSNSSQERFDLIRDPILARVEIATLAI
Human V1aR      1  MRLSAGPDAGPSGNSSPWPLATGAGNTSREAEALGEGNGHFRVVRNDELAKVEIAVLAV
Human V1bR      1  -----MDSGPIIDAN-----PTPRGTLAPNATFDLWLCRDEELAKVEICVLAT
Human OTR       1  -----MEGALAANMSAEAANA SAAPP GAEG--NRTAGPPPRNDALARVEIAVLCI

Lasius INTR      41  IFLVTLIGNTLILFLIYARREYOR-RKFTRMVEFILHLSADLLTGLLDVLPOLAWDITE
Tribolium INTR  37  IFLVTVIGNSTVLLALWTRRRYAGRKLSRMVEFILHLSADLLTGLLDVLPOLAWDITY
Human V2R       47  VEVAVALSNGLVLLALARRCGR---RGHWAPLEVFICHLCLADLAWALFOVLPOLAWKATD
Human V1aR      61  TVAVAVLIGNSVLLAHRIPR---K--TSRMHLFTRHLSADLAWALFOVLPOLAWDITY
Human V1bR      44  VLVLATGGNLAVLLTIGOLGR---K--FSRMHLFVHLHALTDLAWALFOVLPOLAWDITY
Human OTR       49  ILLALSGNACVLLALRTTRQ---K--HSRLFEFMRHLSADLVVAVFOVLPOLAWDITE

Lasius INTR      100  RDGGAVLCKLVKFCGPFVYLSSYVLTVTAMDRYVAICHFLYCSITSRK-SKMMVYGA
Tribolium INTR  97  REYGGHLLCKVVKYGCITLCPYLSSYVLTATAIDRHCAICVPIYCSWISRR-SKVMVYLA
Human V2R       104  RRRGPHALCKAVKYLQMVGMVYASSYVLTAMIDRRHRAICRMLAYRHCSGAHNRRVYVA
Human V1aR      116  RRRGPHALCKAVKYLQVGMVYASSYVLTAMIDRRHRAICRMLAYRHCSGAHNRRVYVA
Human V1bR      99  RRRGPHALCKAVKYLQVGMVYASSYVLTAMIDRRHRAICRMLAYRHCSGAHNRRVYVA
Human OTR       104  RRYGPDLLCRVVKYLVQVGMVYASSYVLLIIMSLEDRCLALCPLRSIRRRID---RLAWLAT

Lasius INTR      159  WIIAAALICVPOVFIFSYCFIS--FGVWECWAFYLYKYGFRAYVTWYSIMOBLLIFVIVY
Tribolium INTR  156  WVASIAFCIPOLIFWYTSVG--EDEYDCWAFQFIPWCKRAYVTWYSISVFMVFLVHIF
Human V2R       164  WAFSLILSLPOLIFFAQENVEGGSGVDCWAFQFAPWGRITVYVTWIALVVEVATLGLIAA
Human V1aR      175  WLSFVLSLTPCYVDFSMLEVNNVTKARDCWAFQFQWGSRAYVTWIMGGIFVAPVVIIGT
Human V1bR      158  WIIAAALISLPOVFIFSLREVIQGSGVDCWAFQFQWGRAYVTWITLAIFFVLPVITLTA
Human OTR       161  WILGIVASAPQVHIFSIREVA--DGVDCWAFQFQWGRAYVTWITLAVYVLPVITLTA

Lasius INTR      217  TYTKICIALITSSKMSGVVDLK-----KNNKANFSOR-----NREELISKAMM
Tribolium INTR  214  TYTSICIEIQQSSSSL---R-----RSSOKSAFC-----KRTFLISRAKI
Human V2R       224  CQVLEIREIHASVPGPSEPRGG--RR-----RGRRTGSEFC-----EGAHVSEAVA
Human V1aR      235  CQGFICQYNTWCNVECKIASRQSKGAE-----QAGVAFQKCFLLAPCVSSVKISIRAKI
Human V1bR      218  CYSLIGHEICKNKIKVKTQAWRVGGGWRTWDRSPSTLAATIRGLPSRVSSINTISRAKI
Human OTR       219  CYGLISFKIWCNTRIKTAAAAAA-----EAEAGAAAGDGCGRVALARVSSVRLISRAKI

Lasius INTR      260  NIVRCHIVITVLYIATSEPHIGSMLWATWDLKAFITLPPFTGAAFWLISLNSITSCVNPW
Tribolium INTR  253  NIVKCHIAVIVMYIACSTPEILACLWATWDEPS---PFIDGPVFWLITLISLNSCCNPW
Human V2R       268  KIVRMLIVIVVYVLCWAPFELVQLWAWDEEAL-L-EGA---PEVILMLLASLNSCCNPW
Human V1aR      288  RTVKMTEVIVLAYIWCWAPFELQMWVWDEMSVW-TESENPTLITLIGSLNSCCNPW
Human V1bR      278  RTVKMTEVIVLAYIWCWAPFELQMWVWDEKNAED-EDSTNVATISMLLGNLNSCCNPW
Human OTR       272  RTVKMTEVIVLAYIWCWAPFELQMWVWDEANAK-DAE---AEIVMLLASLNSCCNPW

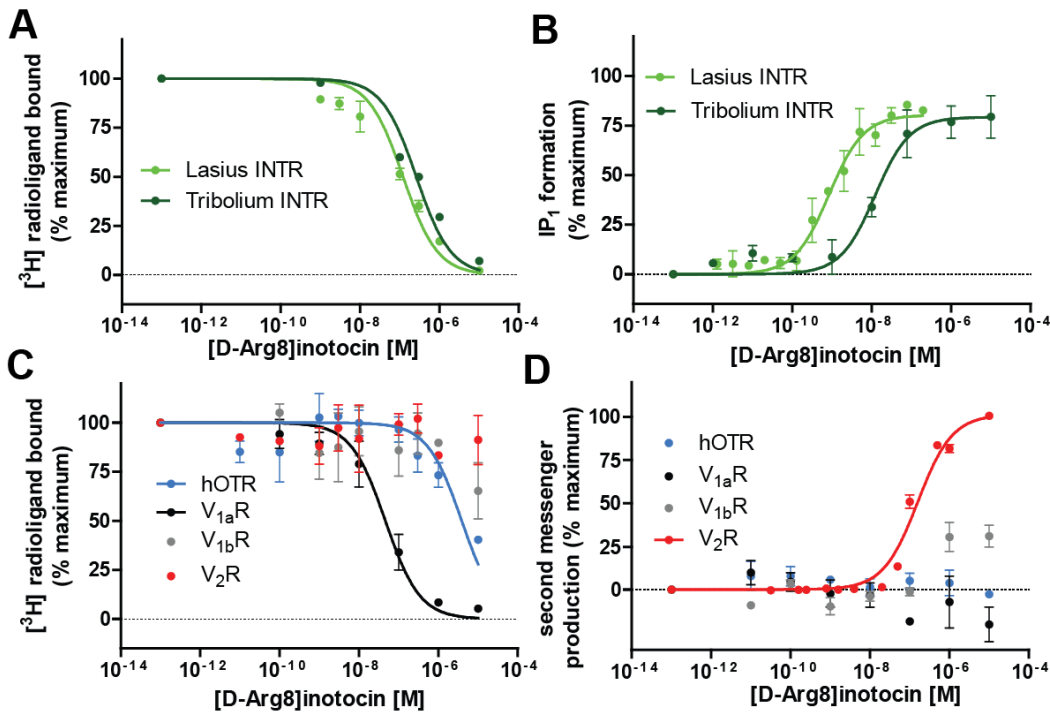
Lasius INTR      320  IYFAFNKEIRGALTNELRYKKDSL-NYDIDARQNV----SDVASTTSSFISR---ISRL
Tribolium INTR  310  IYLAFNREIPRLLRHYTASSK---NYSATGGNSASNSGDAOSTSLRIFSR---WSLC
Human V2R       324  IYASFSSVSSE-IRSLICCARGRTPPSLGPQDESCTTASSSLAKDTSS-----
Human V1aR      347  IYMEFSGHILQDCVQSPCCQNMKEKENKEDTD-SMSRR-QTFYSNNPSITNS-----
Human V1bR      337  IYMGFNSHILPRELRHLACCGGQPRMRRRLSDGSSSRHTLLIRSR-PAATLSLSISLT
Human OTR       328  IYMLTIGHILFHELVCORRLCCSASYLGRRL-GETSASKKNS-----SSFV

Lasius INTR      371  AS--SKIFG-----
Tribolium INTR  364  NSARSNKYPTRVPHFLYVAQYNARRWIVTTT-----
Human V2R       398  -----TGMWKDSPKSSKSIKFIPIVST
Human V1aR      397  ISGRPR--PE---ESPR-----DLELADGEGTAETIIF-----
Human V1bR      373  ISHRS--SQRSCSCLP-----TA-----
Human OTR

```

Supplementary Fig. 2. Multiple sequence alignments between inotocin receptors (*L. niger*, *T. castaneum*) and human V₂R, V_{1a}R, V_{1b}R and OTR. FASTA sequences were aligned through Clustal Omega and shown in Boxshade format. Colour coding is defined as follows: residues that are similar but non-identical are highlighted in grey; identical residues are highlighted in black.

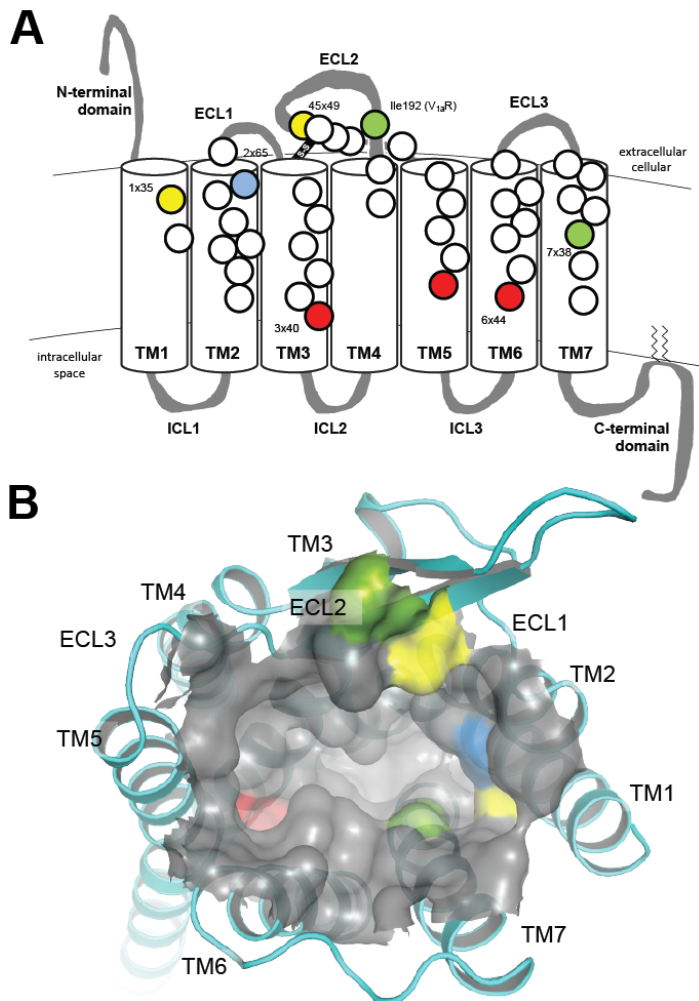
Deleted: S1



44
45
46
47
48
49
50
51
52
53
54
55
56
57
58
59
60
61
62
63
64

Supplementary Fig. 3. Receptor pharmacology of [D-Arg8]-inotocin at inotocin and human oxytocin/vasopressin receptors. (A) Concentration-dependent displacement binding curves of inotocin at inotocin receptors (INTR) from *Lasius niger* (●) ($n = 2$), *Tribolium castaneum* (●) ($n = 3$). (B) Concentration-response curves of [D-Arg8]-inotocin at INTR from *L. niger* ($n = 4$) and *T. castaneum* ($n = 3$) through quantitation of increased intracellular IP₁. (C) Concentration-dependent displacement binding curves of inotocin at human OTR (●), V_{1a}R (●), V_{1b}R (●) and V₂R (●) ($n = 3$). (D) Concentration-response curves of [D-Arg8]-inotocin at human OTR, V_{1a}R, V_{1b}R and V₂R ($n \geq 3$). Specific binding was calculated by subtraction of non-specific binding from total binding and normalized to the percentage (%) of maximal binding. Detailed descriptions of radioligand concentrations, membranes expressing receptors and dissociation constants are provided in the Methods section. Receptor activation was measured by IP₁ assays for the G_q-coupled receptors (human OTR, V_{1a}R, V_{1b}R) and luciferase reporter assay with specific CRE response element for the G_s-coupled human V₂R, as described in Methods. Each data point was normalized to percentage of maximal activation, detected at the highest endogenous ligand concentration, being inotocin for INTR, vasopressin for V_{1a}R, V_{1b}R, V₂R and oxytocin for OTR. Data is shown as mean \pm SEM and fitted by nonlinear regression (sigmoidal, three-parameters, Hill slope of 1).

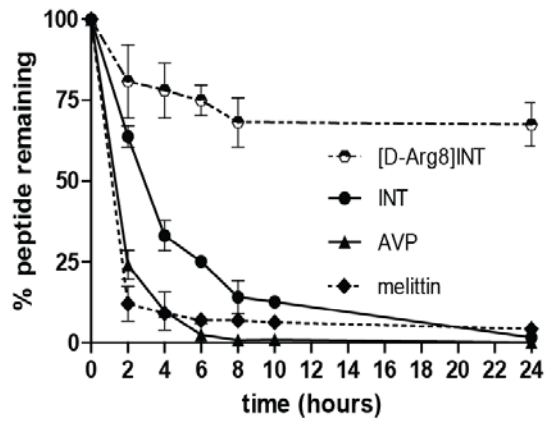
- Deleted: .
- Deleted: S2
- Deleted: a
- Deleted: b
- Deleted: c
- Deleted: d
- Deleted: (●)
- Deleted: (●)
- Deleted: (●)
- Deleted: (●)
- Deleted: Binding of [³H]-inotocin to membrane preparations (10 μg) expressing inotocin receptor from *L. niger* ($n = 2$) or *T. castaneum* ($n = 3$), respectively, were assayed for displacement with an excess of [D-Arg8]-inotocin.
- Deleted: ;
- Deleted: 100% refers on average to 0.65 and 0.69 pmoles of ligand bound per milligram of membrane for inotocin receptor from *L. niger* and *T. castaneum*, respectively. For the displacement bindings at the human receptors, binding of [³H]-vasopressin and [³H]-oxytocin were performed with a radioligand concentration dependent on the K_d of each receptor subtype (1.5, 0.6, 0.1 and 1.2 nM for OTR, V_{1a}R, V_{1b}R and V₂R, respectively). Membrane preparations (30-50 μg) expressing hOTR, V_{1a}R, V_{1b}R and V₂R, respectively were assayed for displacement with an excess of [D-Arg8]inotocin ($n = 3$); 100% refers on average to 0.49, 0.16, 0.36, 0.81 pmoles of ligand bound per milligram of membrane for hOTR, hV_{1a}R, hV_{1b}R and hV₂R, respectively.
- Deleted: Independent experiments were for inotocin receptor *L. niger* ($n = 4$), for inotocin receptor *T. castaneum* ($n = 3$).
- Deleted: hill



109
110
111
112
113
114
115
116
117
118
119
120
121
122
123
124

Supplementary Fig. 4. Structural representation of the human $V_{1a}R$ homology model binding site. (A) 2-dimensional cartoon representation of receptor structure showing relative positions of residues identified from sequence and structural alignments to comprise the predicted binding pocket (circles). Key residues predicted to discriminate the binding and function of inotocin and [D-Arg8]-inotocin are highlighted (coloured circles). Potential binding residues of Arg8/D-Arg8 are shown in yellow; proposed Lys in V_2R that impairs inotocin binding is shown in blue; proposed residues of the activation triad are shown in red; residues in [human \$V_{1b}R\$](#) , V_2R , OTR that potentially impair D-Arg8 binding are presented in green. (B) Van der Waals surface (grey transparent surface) of the binding site residues highlighted in panel A) is presented in the $V_{1a}R$ homology model (cyan cartoon). One continuous cavity is observed within the upper part of the transmembrane domain comprised of 43 residue positions in TM1-7 and ECL1-2.

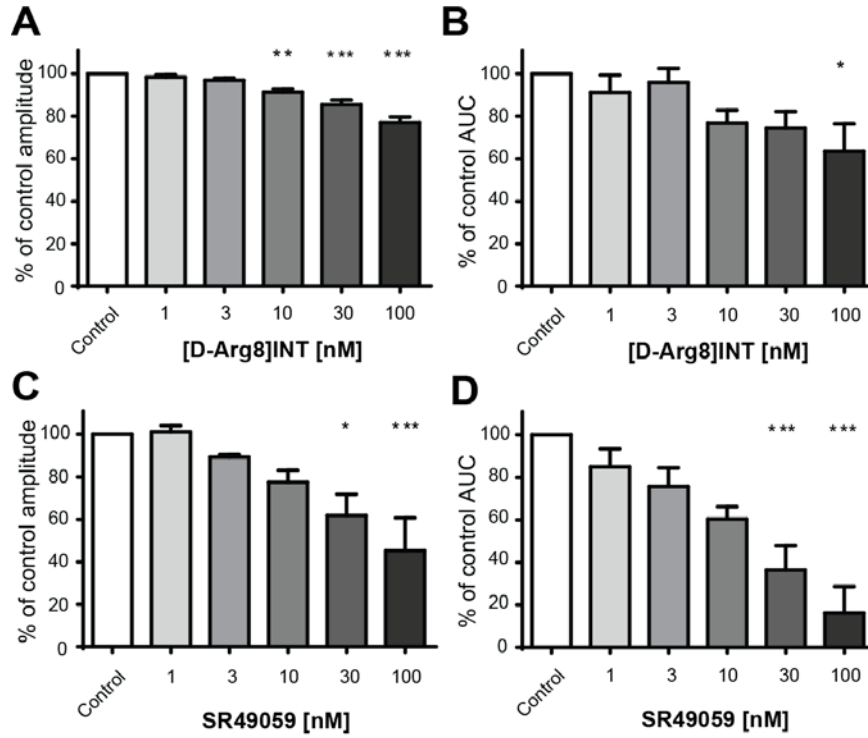
Deleted: S3



126
127
128
129
130
131
132
133
134
135
136

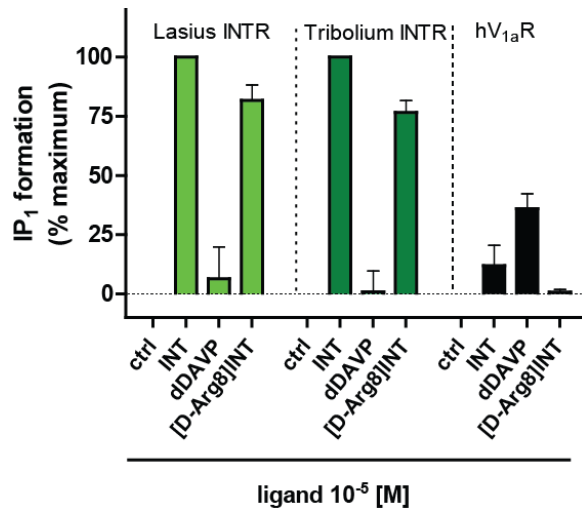
Supplementary Fig. 5. Human serum stability of the inotocin D-analogue. [D-Arg8]-inotocin ([D-Arg8]INT), inotocin (INT), vasopressin (AVP) and melittin (100 μM) were incubated in human serum and their stability monitored via HPLC over a time course of 2, 4, 6, 8, 10 and 24 h. Melittin, a haemolytic peptide from the bee venom was used as a positive control for peptide degradation. Area under the curves of samples was determined and correlated to the negative control analyte, which was dissolved in 0.1% TFA; thus they were not subject to degradation and were assumed therefore as 100%. Peptide stability was expressed in percentage of peptide remaining.

Deleted: S4



139
140
141
142
143
144
145
146
147
148

Supplementary Fig. 6. Concentration-dependent inhibitory effects of [D-Arg8]-inotocin and SR49059 on vasopressin-augmented (0.5 nM) ex vivo uterine contractions. Under [D-Arg8]-inotocin, contraction amplitude was significantly reduced at 10, 30 and 100 nM (A) whilst area-under-the-curve (AUC) was significantly reduced at 100 nM (B). Following treatment with SR49059, amplitude of contraction and AUC were significantly reduced at 30 nM and 100 nM (C and D, respectively); * $P < 0.05$, ** $P < 0.01$, *** $P < 0.001$ ($n = 5$, one-way ANOVA, Tukey's post hoc analysis).



149
150
151
152
153
154
155
156
157
158

Supplementary Fig. 7. Desmopressin is inactive at the insect receptors. Functional second messenger quantification (IP₁ formation) on CHO cells transiently expressing inotocin receptors (INTR) of *L. niger* and *T. castaneum*, respectively, and HEK293 cells expressing human V_{1a}R. The effect of [D-Arg8]-inotocin was analysed in comparison to endogenous inotocin and desmopressin (1-desamino-8-D-arginine vasopressin, dDAVP), carrying also a D-aa analogue in position 8 (n = 3). Cells were treated with 10 μM of each peptide.

Deleted: S5

160 | **Supplementary References**

161 |

162 | 1 Pitti, T. & Manoj, N. Molecular evolution of the neuropeptide S receptor. *PLoS One* 7, e34046, (2012).

163 |